mathematics

MDPI

Article

Stationary Probability Density Analysis for the Randomly Forced Phytoplankton–Zooplankton Model with Correlated Colored Noises

Yuanlin Ma [1] and Xingwang Yu [2,*]

[1] School of Economics, Zhengzhou University of Aeronautics, Zhengzhou 450046, China; mylin446@zua.edu.cn
[2] School of Management Engineering, Zhengzhou University of Aeronautics, Zhengzhou 450046, China
* Correspondence: xwyu2006@zua.edu.cn

Abstract: In this paper, we propose a stochastic phytoplankton–zooplankton model driven by correlated colored noises, which contains both anthropogenic and natural toxins. Using Khasminskii transformation and the stochastic averaging method, we first transform the original system into an Itô diffusion system. Afterwards, we derive the stationary probability density of the averaging amplitude equation by utilizing the corresponding Fokker–Planck–Kolmogorov equation. Then, the stability of the averaging amplitude is studied and the joint probability density of the original two-dimensional system is given. Finally, the theoretical results are verified by numerical simulations, and the effects of noise characteristics and toxins on system dynamics are further illustrated.

Keywords: stochastic phytoplankton–zooplankton model; stationary probability density; stochastic averaging method

MSC: 37H30; 60E05

Citation: Ma, Y.; Yu, X. Stationary Probability Density Analysis for the Randomly Forced Phytoplankton–Zooplankton Model with Correlated Colored Noises. *Mathematics* **2022**, *10*, 2383. https://doi.org/10.3390/math10142383

Academic Editor: Ivo Siekmann

Received: 4 June 2022
Accepted: 4 July 2022
Published: 7 July 2022

1. Introduction

Phytoplankton are tiny floating plants, usually single-celled algae, which sit at the bottom of the food chain and thus support secondary and tertiary productivity in the ocean [1–3]. As the major primary producers in the marine ecosystem, phytoplankton are not only a basic food source for zooplankton, but also provide large amounts of oxygen for humans and other animals after absorbing nearly half of the universal carbon dioxide through photosynthesis [4–6]. However, unfortunately, the rapid and sustained growth of phytoplankton biomass can alter energy flows and disrupt the normal functioning of marine ecosystem [7]. Especially in the stage of algal bloom demise, the decomposition process after the death of high concentration algae can absorb a large amount of dissolved oxygen in the water, resulting in the death of marine organisms asphyxiation, which in turn affects the water quality, tourism, and fishery resources [8,9].

There are many factors that contribute to algal blooms, such as nutrient level [10], temperature [11] and light availability [12], but the key cause for the formation of algal blooms is still not fully understood. Perhaps the main reason behind population succession and algal blooms is the toxins produced by toxin-producing phytoplankton (TPP). For this reason, Chattopadhayay et al. [13] proposed a general form of phytoplankton–zooplankton interaction model with TPP, and concluded that TPP may act as a biological control for planktonic blooms through the field-collected samples and theoretical analysis. Since then, a large number of plankton models with TPP have been developed, with similar results—including, but not limited to, Refs. [14–19]. Notably, most studies only consider the impact of toxic substances released by TPP on the grazing pressure of zooplankton, while ignoring the impact of anthropogenic toxins in the environment. In fact, chemical toxins widely exist in earth's ecosystem as a result of multitudes of human activities, seriously affecting the

survival of plankton and human health [20]. Assuming that prey and predator have different rates of exposure to anthropogenic toxins, Das et al. [21] investigated the bioeconomic harvesting of a prey–predator model in the presence of toxicity. Later, Chakraborty and Das [22] extended this model to three-dimensional case, which includes two-zooplankton and one-phytoplankton. To study the direct and indirect effects of anthropogenic toxins on competitive species, Shan and Huang [23] established a toxin-dependent competition model and found that the level of toxins and the distinct vulnerabilities of two species to toxins can influence competition outcomes in many counterintuitive ways.

Note that the aforementioned models are based on a deterministic approach. Species concentrations, however, are susceptible to fluctuations in the real environment that can not be neglected when seeking a better understanding of the dynamics of complex living systems [24–32]. This is especially true for marine organisms due to the unpredictability of water temperature, nutrient availability, photosynthetically active radiation and other physical factors embedded in aquatic ecosystems [33–36]. Consequently, nonlinear stochastic ecosystem with noise term has recently attracted the attention of scholars [37–41]. For example, authors of [42,43] established different Itô type stochastic plankton models and studied their asymptotic behavior and stability by Lyapunov function method. Significantly, Gauss white noise in the sense of Itô is regarded as ideal white noise with infinite power, which does not exist in reality. As a result, researchers [44] used Stratonovich type stochastic differential equation instead of Itô type to characterize the interaction between plankton and marine environment. In particular, Spagnolo and his co-workers [45–47] developed different types of stochastic population models with multiplicative white Gaussian noise to simulate the complex dynamic behavior of ecosystems and observed that theoretical results can effectively reproduce experimental data. Huang et al. [48] explored bifurcation dynamics of two competing algal species by constructing a stochastic nonlinear model with multiplicative and additive noises. Except for biomathematics, multiplicative and additive noises are also widely used in other many fields, such as medicine [49], physics [50], neurology [51], and signal processing [52]. It is important to note that the above stochastic models were established based on the assumption that noises have different sources, i.e., they are independent of each other. Meanwhile, the researchers [53] uncovered that in some cases noises may have a common source and therefore can be correlated. Although the correlation time of actual noises may be small physically, it can never be strictly zero [54]. Especially, it is important to consider the non-zero correlation time when the fluctuation is large and the driving process relaxation time scale is long [55]. Noise is generally considered harmful and can cause disturbance of the dynamical system. However, in recent years, the constructive and counterintuitive role of noise in nonlinear system, such as noise-enhanced stability [56], noise-induced resonance [57], noise-induced transport [58], etc., has been widely studied theoretically and experimentally. For more information, please refer to Refs. [59–62].

Inspired by the above discussion, it is more reasonable to incorporate natural and anthropogenic toxins and environmental noises into the plankton model. To this end, a randomly forced phytoplankton–zooplankton model driven by correlated colored noises, which contains both anthropogenic and natural toxins, is constructed in Section 2. In Section 3, to explore the stochastic dynamic properties of the model, we first transform the original model into an averaging Itô diffusion system by using the Khasminskii transformation [63] and stochastic averaging method [64,65]. Then, the stationary probability density of the averaging amplitude equation by utilizing the corresponding Fokker–Planck–Kolmogorov equation is derived. Afterwards, the stability of the averaging amplitude is studied and the joint probability density of the proposed two-dimensional system is given. In Section 4, some numerical simulations are carried out to illustrate the obtained theoretical results and the effects of noise characteristics and toxins on system dynamics are further illustrated. Finally, we conclude the paper by a brief discussion in Section 5.

2. Model Formulation

Let $P \equiv P(t)$ and $Z \equiv Z(t)$, respectively, denote the TPP and zooplankton populations at time t. Now some assumptions for establishing the model are presented.

(i) In the absence of zooplankton, the growth of TPP population follows the logistic law with intrinsic growth rate r and environmental carrying capacity K.

(ii) In the absence of limiting factors, the chance of an individual zooplankton encountering prey is proportional to its abundance, so the predation rate is assumed to obey the simple law of mass action. On the other hand, no matter how large the TPP population is, each zooplankton individual has a maximum consumption rate. Therefore, in the presence of toxic algae, the more common choice is the Holling type II functional response to describe this grazing phenomena [13].

(iii) TPP population is directly affected by anthropogenic toxins, while zooplankton population feeding on contaminated TPP is indirectly affected by toxins [21].

(iv) Some external factors such as temperature and climate affect the biological individual, which result in a multiplicative noise $\xi(t)$ [52], while internal factors such as competition between individuals for food and living environment may alter the population directly, leading to an additive noise $\eta(t)$ [53].

Based on the above assumptions, the stochastic phytoplankton–zooplankton model with TPP is given as follows:

$$\begin{cases} \frac{dP}{dt} = rP\left(1 - \frac{P}{K}\right) - \alpha_1 PZ - \gamma_1 P^3 + P\xi(t) + \eta(t), \\ \frac{dZ}{dt} = \alpha_2 PZ - \mu Z - \frac{bPZ}{a+P} - \gamma_2 Z^2 + Z\xi(t) + \eta(t). \end{cases} \tag{1}$$

Worth noting that phytoplankton and zooplankton have different exposure rates to anthropogenic toxins released by external environment due to their density and size. Hence, the effect of anthropogenic toxins on zooplankton population is less than that on TPP population by assumption (iii), namely, the coefficients of toxicity satisfy $0 < \gamma_2 < \gamma_1$ [22]. In addition, both phytoplankton and zooplankton are assumed to be affected by the same multiplicative noise source $\xi(t)$ and the same additive noise source $\eta(t)$, where $\xi(t)$ and $\eta(t)$ are correlated Gaussian colored noises with zero mean and satisfy

$$\begin{aligned} \langle \xi(t)\xi(s) \rangle &= \frac{D_1}{\tau_1} \exp(-\frac{|t-s|}{\tau_1}), \\ \langle \eta(t)\eta(s) \rangle &= \frac{D_2}{\tau_2} \exp(-\frac{|t-s|}{\tau_2}), \\ \langle \xi(t)\eta(s) \rangle &= \frac{D_3}{\tau_3} \exp(-\frac{|t-s|}{\tau_3}). \end{aligned} \tag{2}$$

Here, τ_i $(i = 1, 2, 3)$ denote the correlation time, D_1 and D_2 are the intensity of the two colored noises, and $D_3 = \lambda\sqrt{D_1 D_2}$, where λ represents the correlation degree between the two noises with $|\lambda| < 1$. Biological explanations of other parameters are shown in Table 1. In the following, the stationary probability density of model (1) will be presented.

Table 1. Biological explanation of parameters in model (1).

Parameter	Description
r	Intrinsic growth rate of TPP population
K	Environmental carrying capacity of TPP population
α_1	Rate of predation of zooplankton on TPP population
α_2	Ratio of biomass consumed by zooplankton for its growth
μ	Mortality rate of zooplankton
a	Half saturation constant
b	Rate of toxin liberation by TPP population
γ_1	Coefficient of toxicity to phytoplankton
γ_2	Coefficient of toxicity to zooplankton

3. Stochastic Analysis of The Model

Without considering the impact of noise, model (1) degenerates into a deterministic one. Then the equilibria for the deterministic model is $E_0(0,0)$, $E_1(P_1,0)$, $E_*(P_*,Z_*)$, where

$$P_1 = \frac{1}{2\gamma_1}(-\frac{r}{K} + \sqrt{(\frac{r}{K})^2 + 4r\gamma_1}), Z_* = \frac{1}{\alpha_1}(r - \frac{r}{K}P_* - \gamma_1 P_*^2),$$

and P_* satisfies

$$d_0 P_*^3 + d_1 P_*^2 + d_2 P_* + d_3 = 0, \tag{3}$$

here

$$\begin{aligned} d_0 &= \gamma_1\gamma_2, \\ d_1 &= \alpha_1\alpha_2 + \gamma_2(a\gamma_1 + rK^{-1}), \\ d_2 &= ar\gamma_2K^{-1} - r\gamma_2 + a\alpha_1\alpha_2 - \mu\alpha_1 - b\alpha_1, \\ d_3 &= -a\mu\alpha_1 - ar\gamma_2. \end{aligned}$$

It is obvious from (3) that the necessary and sufficient condition for the existence of positive equilibrium E_* is

$$r - rP_*K^{-1} - \gamma_1 P_*^2 > 0. \tag{4}$$

Next, the stationary probability density and stability of model (1) are discussed in detail. We first introduce a transformation of variables, $X = P - P_*$, $Y = Z - Z_*$, and substitute this into model (1), which will lead to the following form by ignoring the higher powers:

$$\begin{cases} \frac{dX}{dt} = a_{11}X + a_{12}Y + (X + P_*)\xi(t) + \eta(t), \\ \frac{dY}{dt} = a_{21}X + a_{22}Y + (Y + Z_*)\xi(t) + \eta(t), \end{cases} \tag{5}$$

where

$$\begin{aligned} a_{11} =& -rK^{-1}P_* - 2\gamma_1 P_*^2, a_{12} = -\alpha_1 P_*, \\ a_{21} =& \alpha_2 Z_* - \frac{abZ_*}{(a + P_*)^2}, a_{22} = -\gamma_2 Z_*. \end{aligned} \tag{6}$$

It follows from the Khasminskii transformation $X = \rho\cos\theta$ and $Y = \rho\sin\theta$ [63] that

$$\begin{cases} \frac{d\rho}{dt} = f_1(\rho,\theta) + g_{11}(\rho,\theta)\xi(t) + g_{12}(\rho,\theta)\eta(t), \\ \frac{d\theta}{dt} = f_2(\rho,\theta) + g_{21}(\rho,\theta)\xi(t) + g_{22}(\rho,\theta)\eta(t), \end{cases} \tag{7}$$

where

$$\begin{aligned} &f_1(\rho,\theta) = \rho(a_{11}\cos^2\theta + (a_{12} + a_{21})\sin\theta\cos\theta + a_{22}\sin^2\theta), \\ &f_2(\rho,\theta) = a_{21}\cos^2\theta - a_{12}\sin^2\theta + (a_{22} - a_{11})\sin\theta\cos\theta, \\ &g_{11}(\rho,\theta) = \rho + P_*\cos\theta + Z_*\sin\theta, g_{12}(\rho,\theta) = \cos\theta + \sin\theta, \\ &g_{21}(\rho,\theta) = \rho^{-1}(Z_*\cos\theta - P_*\sin\theta), g_{22}(\rho,\theta) = \rho^{-1}(\cos\theta - \sin\theta). \end{aligned} \tag{8}$$

After applying the stochastic averaging method [64,65] for system (7), we obtain

$$\begin{cases} d\rho = m_\rho(\rho)dt + \sigma_{11}(\rho)dw_\rho + \sigma_{12}(\rho)dw_\theta, \\ d\theta = m_\theta(\rho)dt + \sigma_{21}(\rho)dw_\rho + \sigma_{22}(\rho)dw_\theta. \end{cases} \tag{9}$$

Here, w_ρ and w_θ stand for independent standard Wiener processes, and the drift and diffusion coefficients are

$$\begin{aligned}
m_\rho(\rho) =& \frac{1}{2}\rho(a_{11}+a_{22}) + \frac{D_1(2\rho^2\tau_1^2+2\rho^2+P_*^2+Z_*^2)}{2\rho(\tau_1^2+1)} \\
&+ \frac{D_2}{\rho(\tau_2^2+1)} + \frac{D_3(P_*+Z_*)}{\rho(\tau_3^2+1)}, \\
m_\theta(\rho) =& \frac{1}{2}(a_{21}-a_{12}), \sigma_{12}^2(\rho)=0, \sigma_{21}^2(\rho)=0, \\
\sigma_{11}^2(\rho) =& \frac{D_1(2\rho^2\tau_1^2+2\rho^2+P_*^2+Z_*^2)}{\tau_1^2+1} + \frac{2D_2}{\tau_2^2+1} + \frac{2D_3(P_*+Z_*)}{\tau_3^2+1}, \\
\sigma_{22}(\rho) =& \frac{D_1(P_*^2+Z_*^2)}{\rho^2(\tau_1^2+1)} + \frac{2D_2}{\rho^2(\tau_2^2+1)} + \frac{2D_3(P_*+Z_*)}{\rho^2(\tau_3^2+1)}.
\end{aligned}$$

For simplicity, we introduce some notations:

$$\begin{aligned}
&\varphi_1 = \frac{1}{2}(a_{11}+a_{22}) + D_1, \varphi_2 = 2D_1, \varphi_3 = \frac{1}{2}(a_{21}-a_{12}), \\
&\varphi_4 = \frac{D_1(P_*^2+Z_*^2)}{2(\tau_1^2+1)} + \frac{D_2}{\tau_2^2+1} + \frac{D_3(P_*+Z_*)}{\tau_3^2+1}.
\end{aligned} \tag{10}$$

Then the probability density function $p(\rho)$ for the diffusion process (ρ, θ) satisfies the Fokker–Planck–Kolmogorov equation

$$\frac{\partial p}{\partial t} + \frac{\partial}{\partial \rho}(m_\rho p) + \frac{\partial}{\partial \theta}(m_\theta p) = \frac{1}{2}\Big[\frac{\partial^2}{\partial \rho^2}(\sigma_{11}^2 p) + \frac{\partial^2}{\partial \theta^2}(\sigma_{22}^2 p)\Big]. \tag{11}$$

Note that the amplitude ρ in (9) does not depend on the phase θ, so Equation (11) degenerates into

$$\frac{\partial p}{\partial t} = -\frac{\partial}{\partial \rho}(m_\rho p) + \frac{1}{2}\frac{\partial^2}{\partial \rho^2}(\sigma_{11}^2 p), \tag{12}$$

i.e.,

$$\frac{\partial p}{\partial t} = -\frac{\partial}{\partial \rho}[(\varphi_1\rho + \varphi_4\rho^{-1})p] + \frac{1}{2}\frac{\partial^2}{\partial \rho^2}[(2\varphi_4 + \varphi_2\rho^2)p]. \tag{13}$$

It then follows from $\frac{\partial p}{\partial t} = 0$ that the stationary probability density function $p(\rho)$ satisfies

$$-\frac{\partial}{\partial \rho}[(\varphi_1\rho + \varphi_4\rho^{-1})p] + \frac{1}{2}\frac{\partial^2}{\partial \rho^2}[(2\varphi_4 + \varphi_2\rho^2)p] = 0. \tag{14}$$

From Equations (6) and (10), we know that $\varphi_2 > 0$ and $\varphi_4 > 0$. Therefore, when $\varphi_2 > 2\varphi_1$, the following expression of stationary probability density function can obtained from (14)

$$p(\rho) = \frac{\varphi_2}{\varphi_4}\rho\big(1+\frac{\varphi_2}{2\varphi_4}\rho^2\big)^{\frac{\varphi_1}{\varphi_2}-\frac{3}{2}}\Gamma\big(\frac{3}{2}-\frac{\varphi_1}{\varphi_2}\big)\Gamma^{-1}\big(\frac{1}{2}-\frac{\varphi_1}{\varphi_2}\big), \tag{15}$$

where $\Gamma(x) = \int_0^\infty t^{x-1}e^{-t}dt$ is the Gamma function with $t > 0$.

One can see from $\frac{dp(\rho)}{d\rho} = 0$ that the extreme point of $p(\rho)$ is $\sqrt{\frac{\varphi_4}{\varphi_2-\varphi_1}}$ $(\varphi_2 > 2\varphi_1)$. Further calculations show that $\frac{d^2p(\rho)}{d\rho^2}\big|_{\rho=\sqrt{\frac{\varphi_4}{\varphi_2-\varphi_1}}} < 0$, which implies that $\bar{\rho} = \sqrt{\frac{\varphi_4}{\varphi_2-\varphi_1}}$ $(\varphi_2 > 2\varphi_1)$ is a maximum point of $p(\rho)$. According to Namachchivaya's theory [66], the extreme value of an invariant measure contains the most important essence of nonlinear stochastic system, namely, the sample trajectory will stay near $\bar{\rho}$ with bigger probability, which means that $\bar{\rho}$ is stable in the sense of probability.

According to $\rho = (X^2 + Y^2)^{\frac{1}{2}}$, we can further obtain the following joint probability density of variables X and Y:

$$\Psi(X,Y) = \frac{\varphi_2}{\varphi_4}(X^2+Y^2)^{\frac{1}{2}}\left[1+\frac{\varphi_2}{2\varphi_4}(X^2+Y^2)\right]^{\frac{\varphi_1}{\varphi_2}-\frac{3}{2}}\Gamma\left(\frac{3}{2}-\frac{\varphi_1}{\varphi_2}\right)\Gamma^{-1}\left(\frac{1}{2}-\frac{\varphi_1}{\varphi_2}\right). \tag{16}$$

Hence, $\Psi(X,Y)$ exists a maximum value at the points of the stable limit cycle

$$X^2+Y^2 = \frac{\varphi_4}{\varphi_2-\varphi_1}.$$

For system (1), we can obtain similar results, namely, the probability density of variables P and Z is

$$\Psi(P,Z) = \frac{\varphi_2}{\varphi_4}\sqrt{\Theta(P,Z)}\left[1+\frac{\varphi_2}{2\varphi_4}\Theta(P,Z)\right]^{\frac{\varphi_1}{\varphi_2}-\frac{3}{2}}\Gamma\left(\frac{3}{2}-\frac{\varphi_1}{\varphi_2}\right)\Gamma^{-1}\left(\frac{1}{2}-\frac{\varphi_1}{\varphi_2}\right), \tag{17}$$

where $\Theta(P,Z) = (P-P_*)^2 + (Z-Z_*)^2$.

4. Numerical Simulation

In this section, we will perform some numerical simulations to verify the theoretical results and further illustrate the effects of noise characteristics and anthropogenic and natural toxins on system dynamics. Unless otherwise specified, all numerical simulations in this paper are carried out by fixing parameters $r = 0.2$, $K = 108$, $\alpha_1 = 1$, $\alpha_2 = 0.15$, $\mu = 0.075$, $a = 5.7$ and changing D_i, τ_i, γ_j and b, $i = 1,2,3$, $j = 1,2$.

(i) Assuming that one noise intensity is fixed while the other two change continuously, and selecting $\tau_1 = 0.5$, $\tau_2 = 0.8$, $\tau_3 = 0.1$, $\gamma_1 = 0.057$, $\gamma_2 = 0.02$ and $b = 0.5$, we plot Figure 1, which shows the effect of noise intensity on the maximum amplitude $\bar{\rho}$. We find from Figure 1 that the maximum amplitude $\bar{\rho}$ decreases with the increase in multiplicative noise intensity D_1, but the effect of D_2 and D_3 is just the opposite.

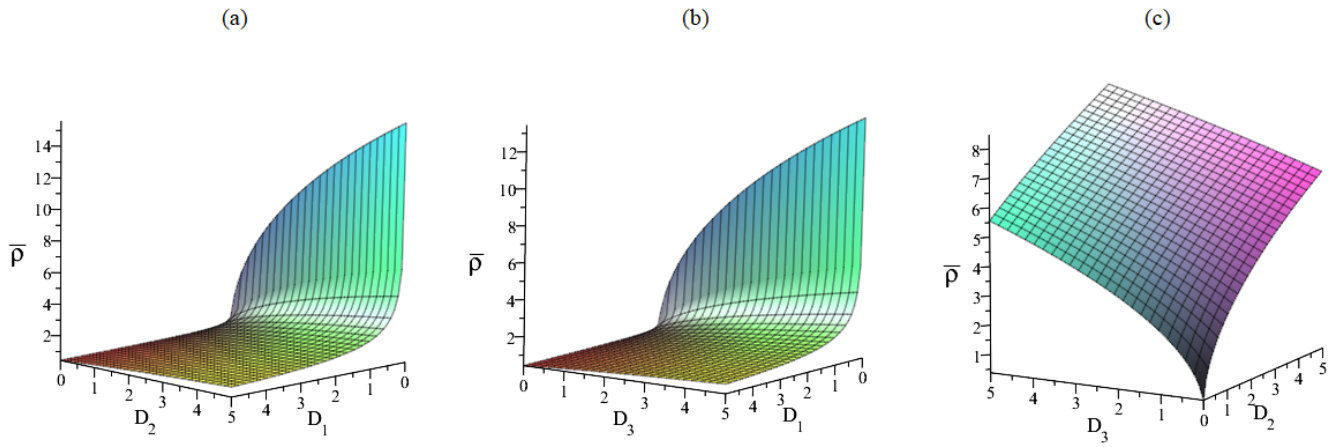

Figure 1. Maximum amplitude $\bar{\rho}$ for different noise intensities, where (**a**) $D_3 = 0.15$, (**b**) $D_2 = 0.05$, (**c**) $D_1 = 0.1$.

(ii) Let $D_1 = 0.1$, $D_2 = 0.05$, $D_3 = 0.15$, $\gamma_1 = 0.057$, $\gamma_2 = 0.02$, $b = 0.5$. Then, the effect of correlation time on the maximum amplitude $\bar{\rho}$ is shown in Figure 2. Clearly, $\bar{\rho}$ tends to decrease due to the increase in τ_i ($i = 1,2,3$), which means that the correlation time is not conducive to the stability of the system.

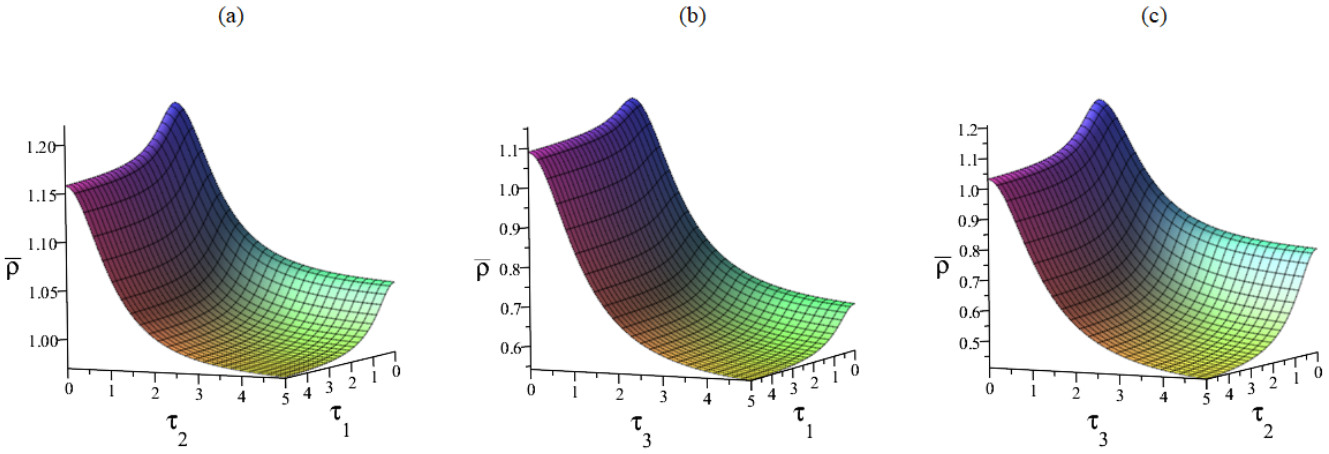

Figure 2. Maximum amplitude $\bar{\rho}$ for different correlation times, where (**a**) $\tau_3 = 0.1$, (**b**) $\tau_2 = 0.8$, (**c**) $\tau_1 = 0.5$.

(iii) Figure 3 is plotted by choosing $D_1 = 0.1$, $D_2 = 0.05$, $D_3 = 0.15$, $\tau_1 = 0.5$, $\tau_2 = 0.8$, $\tau_3 = 0.1$ and $b = 0.5$, which illustrates the effect of anthropogenic toxins. We see from Figure 3 that $\bar{\rho}$ decreases with increasing γ_1, while the effect of γ_2 is more complex. To be specific, $\bar{\rho}$ increases only when γ_2 is smaller and decreases when γ_2 is larger, so γ_2 exists a maximum point. This implies that the coefficient of anthropogenic toxicity to zooplankton γ_2 may be used as a biological control measure for algal blooms.

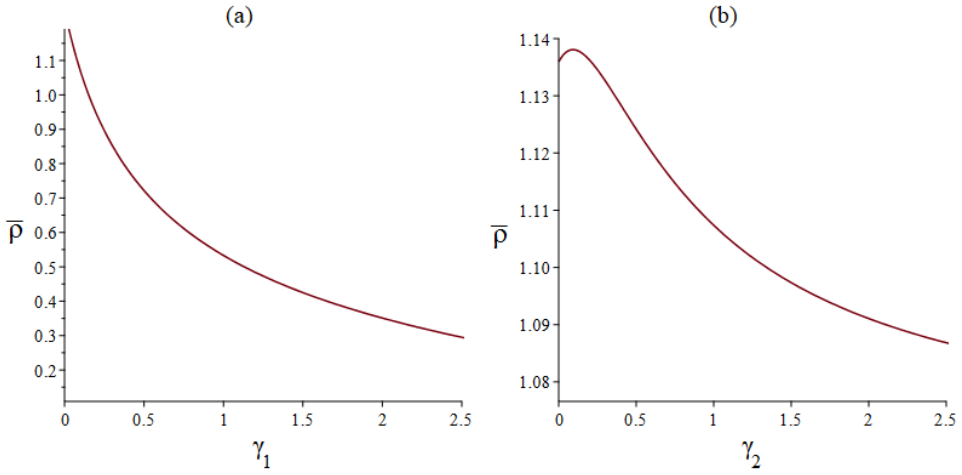

Figure 3. Effect of anthropogenic toxins on maximum amplitude $\bar{\rho}$, where (**a**) $\gamma_2 = 0.02$, (**b**) $\gamma_1 = 0.057$.

(iv) Let $D_1 = 0.1$, $D_2 = 0.05$, $D_3 = 0.15$, $\tau_1 = 0.5$, $\tau_2 = 0.8$, $\tau_3 = 0.1$, $\gamma_1 = 0.057$, $\gamma_2 = 0.02$. Then, the effect of TPP population on the maximum amplitude $\bar{\rho}$, i.e., the effect of natural toxins, is shown in Figure 4. Interestingly, Figure 4 exhibits two extreme values, a maximum and a minimum, and $\bar{\rho} \to \infty$ when $b \to \infty$. That is to say, toxin release rate by TPP population b may affect the intensity of the algal blooms, so it plays an important role in the formation of algal blooms.

(v) Let $D_1 = D_2 = D_3 = 0.01$, $\tau_1 = \tau_2 = \tau_3 = 0.02$, $\gamma_1 = 0.057$, $\gamma_2 = 0.02$, $b = 0.5$. Then, we plot the joint probability density of system (5), as shown in Figure 5. Therefore, $\Psi(X, Y)$ exists a maximum value at the points of the stable limit cycle: $X^2 + Y^2 = \frac{\varphi_4}{\varphi_2 - \varphi_1} = 0.63$.

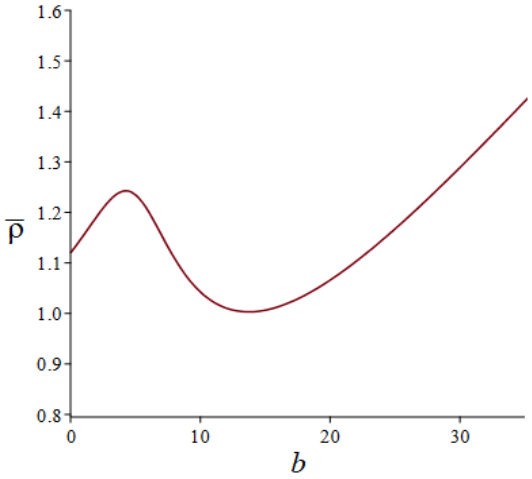

Figure 4. Effect of toxin release rate by TPP population on maximum amplitude $\bar{\rho}$.

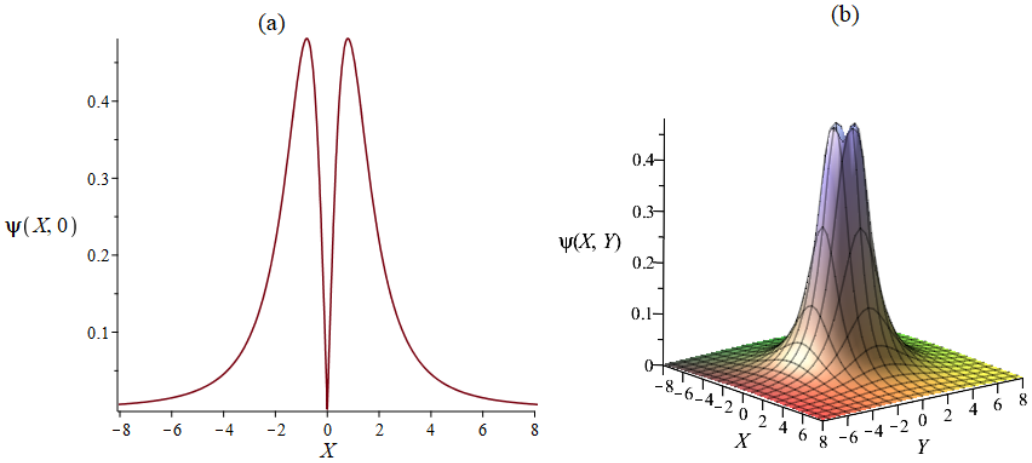

Figure 5. (**a**) Joint probability density $\Psi(X, 0)$ of system (5); (**b**) Joint probability density $\Psi(X, Y)$ of system (5).

5. Discussion

Considering internal and external random factors, in this paper we proposed a stochastic phytoplankton–zooplankton model with correlated colored noises. In order to explore the stochastic dynamics of the model, we first employed the Khasminskii transformation and stochastic averaging method to transform the original model into an averaging Itô diffusion system. Then, the stationary probability density of the diffusion process was obtained by utilizing the corresponding Fokker–Planck–Kolmogorov equation. Finally, we discussed the stability of the averaging amplitude with the help of maximum value and presented the joint probability density of the original two-dimensional system. Summarizing the theoretical and numerical results, we can draw the following interesting conclusions.

- The noise intensity D_1, the correlation time τ_i $(i = 1, 2, 3)$ and the coefficient of anthropogenic toxicity γ_1 may reduce the level of $\bar{\rho}$, namely, the distribution range of population density will be more concentrated with the increase in D_1, τ_i $(i = 1, 2, 3)$, and γ_1. Ecologically, these parameters are favorable for maintaining a balanced plankton population, which may seem counterintuitive.
- The noise intensities D_2 and D_3 can enhance the level of $\bar{\rho}$, which implies that the distribution range of population density will be enlarged with the increase in D_2 and D_3. As a result, they weaken the stability of the system.
- The influence of anthropogenic toxicity coefficient γ_1 and the toxin release rate by TPP population b is more complicated, depending on the content of the two toxins. In other words, these two parameters can be used as a means of controlling algal blooms.

This paper is concerned with stationary probability density analysis for the randomly forced phytoplankton–zooplankton model with correlated colored noises. The obtained results may enrich the research of aquatic ecosystem dynamics. Note here that the model proposed in this paper is a two-dimensional model, which is based on top-down mechanism. How to construct a high-dimensional stochastic food chain model based on both bottom-up and top-down mechanisms to describe the interaction between nutrients and plankton, and to carry out its stationary probability density analysis is a problem worth discussing. We leave this for future investigations.

Author Contributions: Conceptualization, X.Y.; Formal analysis, Y.M.; Funding acquisition, X.Y.; Methodology, X.Y.; Writing—original draft, Y.M. All authors have read and agreed to the published version of the manuscript.

Funding: This work was supported by the National Natural Science Foundation of China (No. 12171441), the Key Scientific Research Project of Colleges and Universities of Henan Province (Nos. 21A110024, 21A460027), and the Key Science and Technology Research Project of Henan Province (No. 222102320432).

Institutional Review Board Statement: Not applicable.

Informed Consent Statement: Not applicable.

Data Availability Statement: Not applicable.

Conflicts of Interest: The authors declare no conflict of interest.

References

1. Bharathi, M.; Venkataramana, V.; Sarma, V. Phytoplankton community structure is governed by salinity gradient and nutrient composition in the tropical estuarine system. *Cont. Shelf. Res.* **2022**, *234*, 104643. [CrossRef]
2. Sekerci, Y.; Petrovskii, S. Mathematical modelling of plankton-oxygen dynamics under the climate change. *Bull. Math. Biol.* **2015**, *77*, 2325–2353. [CrossRef] [PubMed]
3. Agnihotri, K.; Kaur, H. The dynamics of viral infection in toxin producing phytoplankton and zooplankton system with time delay. *Chaos Solitons Fractals* **2019**, *118*, 122–133. [CrossRef]
4. Niu, Y.; Liu, C.; Lu, X.; Zhu, L.; Sun, Q.; Wang, S. Phytoplankton blooms and its influencing environmental factors in the southern Yellow Sea. *Reg. Stud Mar. Sci.* **2021**, *47*, 101916. [CrossRef]
5. Bao, L.; Chen, J.; Tong, H.; Qian, J.; Li, X. Phytoplankton dynamics and implications for eutrophication management in an urban river with a series of rubber dams. *J. Environ. Manag.* **2022**, *311*, 114865. [CrossRef]
6. Ghanbari, B.; Gómez-Aguilar, J. Modeling the dynamics of nutrient-phytoplankton-zooplankton system with variable-order fractional derivatives. *Chaos Soliton. Fract.* **2018**, *116*, 114–120. [CrossRef]
7. Schweigert, J.; Thompson, M.; Fort, C.; Hay, D.E.; Therriault, T.W.; Brown, L.N. Factors linking Pacific herring (Clupea pallasi) productivity and the spring plankton bloom in the Strait of Georgia, British Columbia, Canada. *Prog. Oceanogr.* **2013**, *115*, 103–110. [CrossRef]
8. Niu, L.; Van Gelder, P.; Zhang, C.; Guan, Y.; Vrijling, J.K. Physical control of phytoplankton bloom development in the coastal waters of Jiangsu (China). *Ecol. Model.* **2016**, *321*, 75–83. [CrossRef]
9. Sohma, A.; Imada, R.; Nishikawa, T.; Shibuki, H. Modeling the life cycle of four types of phytoplankton and their bloom mechanisms in a benthic-pelagic coupled ecosystem. *Ecol. Model.* **2022**, *467*, 109882. [CrossRef]
10. Kumar, B.; Bhaskararao, D.; Krishna, P. Impact of nutrient concentration and compositionon shifting of phytoplankton community in the coastal waters of the Bay of Bengal. *Reg. Stud. Mar. Sci.* **2022**, *51*, 102228. [CrossRef]
11. Zhao, Q.; Liu, S.; Niu, X. Effect of water temperature on the dynamic behavior of phytoplankton-zooplankton model. *Appl. Math. Comput.* **2020**, *378*, 125211. [CrossRef]
12. Chen, M.; Fan, M.; Liu, R.; Wang, X.; Yuan, X.; Zhu, H. The dynamics of temperature and light on the growth of phytoplankton. *J. Theor. Biol.* **2015**, *385*, 8–19. [CrossRef] [PubMed]
13. Chattopadhayay, J.; Sarkar, R.R.; Mandal, S. Toxin-producing plankton may act as a biological control for planktonic blooms-field study and mathematical modelling. *J. Theor. Biol.* **2002**, *215*, 333–344. [CrossRef] [PubMed]
14. Pal, R.; Basu, D.; Banerjee, M. Modelling of phytoplankton allelopathy with Monod-Haldane-type functional response-a mathematical study. *Biosystems* **2009**, *95*, 243–253. [CrossRef] [PubMed]
15. Scotti, T.; Mimura, M.; Wakano, J.Y. Avoiding toxic prey may promote harmful algal blooms. *Ecol. Complex.* **2015**, *21*, 157–165. [CrossRef]
16. Jang, S.; Baglama, J.; Wu, L. Dynamics of phytoplankton-zooplankton systems with toxin producing phytoplankton. *Appl. Math. Comput.* **2014**, *227*, 717–740. [CrossRef]

17. Han, R.; Dai, B. Spatiotemporal pattern formation and selection induced by nonlinear cross-diffusion in a toxic-phytoplankton-zooplankton model with Allee effect. *Nonlinear Anal. Real World Appl.* **2019**, *45*, 822–853. [CrossRef]
18. Peng, Y.; Li, Y.; Zhang, T. Global bifurcation in a toxin producing phytoplankton-zooplankton system with prey-taxis. *Nonlinear Anal. Real World Appl.* **2021**, *61*, 103326. [CrossRef]
19. Liu, C.; Yu, L.; Zhang, Q.; Li, Y. Dynamic analysis of a hybrid bioeconomic plankton system with double time delays and stochastic fluctuations. *Appl. Math. Comput.* **2018**, *316*, 115–137. [CrossRef]
20. Walker, C.H.; Sibly, R.M.; Hopkin, S.H.; Peakall, D.B. *Principles of Ecotoxicology*; CRC Press: Boca Raton, FL, USA, 2012.
21. Das, T.; Mukherjee, R.N.; Chaudhuri, K.S. Harvesting of a prey-predator fishery in the presence of toxicity. *Appl. Math. Model.* **2009**, *33*, 2282–2292. [CrossRef]
22. Chakraborty, K.; Das, K. Modeling and analysis of a two-zooplankton one-phytoplankton system in the presence of toxicity. *Appl. Math. Model.* **2015**, *39*, 1241–1265. [CrossRef]
23. Huang, Q.; Wang, H.; Lewis, M.A. The impact of environmental toxins on predator-prey dynamics. *J. Theor. Biol.* **2015**, 378, 12–30. [CrossRef]
24. May, R. *Stability and Complexity in Model Ecosystems*; Princeton University Press: Princeton, NJ, USA, 1973.
25. Qi, H.; Meng, X.; Hayat, T.; Hobiny, A. Stationary distribution of a stochastic predator-prey model with hunting cooperation. *Appl. Math. Lett.* **2022**, *1124*, 107662. [CrossRef]
26. Li, D.; Liu, S.; Cui, J. Threshold dynamics and ergodicity of an SIRS epidemic model with semi-Markov switching. *J. Differ. Equ.* **2019**, 266, 3973–4017. [CrossRef]
27. Liu, M. Optimal harvesting of stochastic population models with periodic coefficients. *J. Nonlinear Sci.* **2022**, *32*, 23. [CrossRef]
28. Song, M.; Zuo, W.; Jiang, D.; Hayat, T. Stationary distribution and ergodicity of a stochastic cholera model with multiple pathways of transmission. *J. Frankl. Inst.* **2020**, *357*, 10773–10798. [CrossRef]
29. Li, X.; Liu, W.; Mao, X.; Zhao, J. Stabilization and destabilization of hybrid systems by periodic stochastic controls. *Syst. Control Lett.* **2021**, *152*, 104929. [CrossRef]
30. He, S.; Tang, S.; Cai, Y.; Wang, W.; Rong, L. A stochastic epidemic model coupled with seasonal air pollution: Analysis and data fitting. *Stoch. Environ. Res. Risk Assess.* **2020**, *34*, 2245–2257. [CrossRef]
31. Nguyen, D.; Yin, G.; Zhu, C. Long-term analysis of a stochastic SIRS model with general incidence rates. *SIAM J. Appl. Math.* **2020**, *80*, 814–838. [CrossRef]
32. Yu, X.; Ma, Y. An avian influenza model with nonlinear incidence and recovery rates in deterministic and stochastic environments. *Nonlinear Dyn.* **2022**, *108*, 4611–4628. [CrossRef]
33. Sarkar, R.R.; Chattopadhayay, J. The role of environmental stochasticity in a toxic phytoplankton-non-toxic phytoplankton-zooplankton system. *Environmetrics* **2003**, *14*, 775–792. [CrossRef]
34. Chen, Z.; Zhang, R.; Li, J.; Zhang, S.; Wei, C. A stochastic nutrient-phytoplankton model with viral infection and Markov switching. *Chaos Solitons Fractals* **2020**, *140*, 110109. [CrossRef]
35. Jang, S.; Allen, E. Deterministic and stochastic nutrient-phytoplankton-zooplankton models with periodic toxin producing phytoplankton. *Appl. Math. Comput.* **2015**, *271*, 52–67. [CrossRef]
36. Song, D.; Fan, M.; Yan, S.; Liu, M. Dynamics of a nutrient-phytoplankton model with random phytoplankton mortality. *J. Theor. Biol.* **2020**, *488*, 110119. [CrossRef] [PubMed]
37. Wang, H.; Jiang, D.; Hayat, T.; Alsaedi, A.; Ahmad, B. Stationary distribution of stochastic NP ecological model under regime switching. *Phys. A* **2020**, *549*, 124064. [CrossRef]
38. Sarkar, R.R.; Chattopadhayay, J. Occurrence of planktonic blooms under environmental fluctuations and its possible control mechanism-mathematical models and experimental observations. *J. Theor. Biol.* **2003**, *224*, 501–516. [CrossRef]
39. Xu, C. Phenomenological bifurcation in a stochastic logistic model with correlated colored noises. *Appl. Math. Lett.* **2020**, *101*, 106064. [CrossRef]
40. Hu, J.; Liu, Z. Incorporating two coupling noises into a nonlinear competitive system with saturation effect. *Int. J. Biomath.* **2020**, *13*, 2050012. [CrossRef]
41. Tian, B.; Yang, L.; Chen, X.; Zhang, Y. A generalized stochastic competitive system with Ornstein-Uhlenbeck process. *Int. J. Biomath.* **2021**, *14*, 2150001. [CrossRef]
42. Liao, T. The impact of plankton body size on phytoplankton-zooplankton dynamics in the absence and presence of stochastic environmental fluctuation. *Chaos Solitons Fractals* **2022**, *154*, 111617. [CrossRef]
43. Yu, X.; Yuan, S.; Zhang, T. The effects of toxin-producing phytoplankton and environmental fluctuations on the planktonic blooms. *Nonlinear Dyn.* **2018**, *91*, 1653–1668. [CrossRef]
44. Zhang, Y.; Zheng, Y.; Zhao, F.; Liu, X. Dynamical analysis in a stochastic bioeconomic model with stage-structuring. *Nonlinear Dyn.* **2016**, *84*, 1113–1121. [CrossRef]
45. Denaro, G.; Valenti, D.; Spagnolo, B.; Basilone, G.; Mazzola, S.; Zgozi, S.W.; Aronica, S.; Bonanno, A. Dynamics of two picophytoplankton groups in mediterranean sea: Analysis of the deep chlorophyll maximum by a stochastic advection-reaction-diffusion model. *PLoS ONE* **2013**, *8*, e66765. [CrossRef] [PubMed]
46. Caruso, A.; Gargano, M.E.; Valenti, D.; Fiasconaro, A.; Spagnolo, B. Cyclic fluctuations, climatic changes and role of noise in planktonic foraminifera in the mediterranean sea. *Fluct. Noise Lett.* **2005**, *5*, L349–L355. [CrossRef]

47. Spagnolo, B.; Cirone, M.; Barbera, A.; de Pasquale, F. Noise-induced effects in population dynamics. *J. Phys-Condens. Mat.* **2002**, *14*, 2247–2255. [CrossRef]
48. Huang, D.; Wang, H.; Feng, J.; Zhu, Z.W. Hopf bifurcation of the stochastic model on HAB nonlinear stochastic dynamics. *Chaos Soliton. Fract.* **2006**, *27*, 1072–1079. [CrossRef]
49. Zeng, C.; Wang, H. Colored noise enhanced stability in a tumor cell growth system under immune response. *J. Stat. Phys.* **2010**, 141, 889–908. [CrossRef]
50. Guarcello, C.; Valenti, D.; Carollo, A.; Spagnolo, B. Stabilization effects of dichotomous noise on the lifetime of the superconducting state in a long Josephson junction. *Entropy* **2015**, *17*, 2862–2875. [CrossRef]
51. Mikhaylov, A.; Pimashkin, A.; Pigareva, Y.; Gerasimova, S.; Gryaznov, E.; Shchanikov, S.; Zuev, A.; Talanov, M.; Lavrov, I.; Demin, V.; et al. Neurohybrid memristive CMOS-integrated systems for biosensors and neuroprosthetics. *Front. Neurosci.* **2020**, *14*, 358. [CrossRef]
52. Wang, K.; Ju, L.; Wang, Y.; Li, S.H. Impact of colored cross-correlated non-Gaussian and Gaussian noises on stochastic resonance and stochastic stability for a metapopulation system driven by a multiplicative signal. *Chaos Solitons Fractals* **2018**, *108*, 166–181. [CrossRef]
53. Fulinski, A.; Telejko, T. On the effect of interference of additive and multiplicative noises. *Phys. Lett. A* **1991**, *152*, 11–14. [CrossRef]
54. Mei, D.; Xie, C.; Zhang, L. The stationary properties and the state transition of the tumor cell growth model. *Eur. Phys. J. B* **2004**, *41*, 107–112. [CrossRef]
55. Madureira, A.J.R.; Haenggi, P.; Wio, H.S. Giant suppression of the activation rate in the presence of correlated white noise sources. *Phys. Lett. A* **1996**, *217*, 248–252. [CrossRef]
56. Mantegna, R.N.; Spagnolo, B. Probability distribution of the residence times in periodically fluctuating metastable systems. *Int. J. Bifurcat. Chaos* **1998**, *8*, 783–790. [CrossRef]
57. Mikhaylov, A.N.; Guseinov, D.V.; Belov, A.I.; Korolev, D.S.; Shishmakova, V.A.; Koryazhkina, M.N.; Filatov, D.O.; Gorshkov, O.N.; Maldonado, D.; Alonso, F.J.; et al. Stochastic resonance in a metal-oxide memristive device. *Chaos Solitons Fractals* **2021**, *144*, 110723. [CrossRef]
58. Li, Y.G.; Xu, Y.; Kurths, J.; Yue, X. Lévy-noise-induced transport in a rough triple-well potential. *Phys. Rev. E* **2016**, *94*, 042222. [CrossRef]
59. Guarcello, C.; Valenti, D.; Spagnolo, B.; Pierro, V.; Filatrella, G. Anomalous transport effects on switching currents of graphene-based Josephson junctions. *Nanotechnology* **2017**, *28*, 134001. [CrossRef] [PubMed]
60. Carollo, A.; Valenti, D.; Spagnolo, B. Geometry of quantum phase transitions. *Phys. Rep.* **2020**, *838*, 1–72. [CrossRef]
61. Ma, Y.; Yu, X. Stochastic stability and stationary probability density analysis for a nutrient-phytoplankton model with multiplicative and additive noises. *Appl. Math. Lett.* **2022**, *132*, 108201. [CrossRef]
62. Yu, X.; Ma, Y. Steady-state analysis of the stochastic Beverton-Holt growth model driven by correlated colored noises. *Chaos Soliton. Fract.* **2022**, *158*, 112102. [CrossRef]
63. Khasminskii, R. On the principle of averaging for Itô stochastic differential equations. *Kybernetika (Prague)* **1968**, *4*, 260–279.
64. Zhu, W. *Nonlinear Stochastic Dynamics and Control Hamilton Theory System Framework*; Science Press: Beijing, China, 2003.
65. Xu, Y.; Guo, R.; Jia, W.; Li, J. Stochastic averaging for a class of single degree of freedom systems with combined Gaussian noises. *Acta Mech.* **2014**, *225*, 2611–2620. [CrossRef]
66. Namachchivaya, N. Stochastic bifurcation. *Appl. Math. Comput.* **1990**, *38*, 101–159.